the value of v increased in discrete integer steps (g_{up}) for excited stores and decreased by discrete integer steps (g_{down}) for recovering stores. We set $g_{up} = 25$ and $g_{down} = 5$. In the equation $\{k_{co}+[r\ (2r + 1) - k_{co}]\ (v/v_{exc})\}$, $k_{co} = 5$ was used to calculate the minimum number of excited neighbors necessary to excite a resting store at v; $k_{ro} = 7$ was used in the equation $\{k_{ro} + [r(2r + 1) - k_{ro}]\ [(v - v_{max}) / (v_{rcc} - v_{max})]\}$ to calculate the minimum number of relaxed neighbors to cause relaxation of an excited store at v. At time zero, a 20 by 20 square of stores was excited ($v = 0$) next to a 20 by 20 recovering square of stores ($v = v_{max}$). This resulted in a stable spiral that had an initial wavelength of 56 stores and a period of 25 iterations. When a single row of stores was stimulated, the plane wave velocity was three stores per iteration. Given the empirically measured spiral period of 10 s and a plane wave velocity of 26 μm/s, this model predicted 0.4 s per iteration and 3.4 μm per store. The predicted initial wavelength of 190 μm differed by less than 10% from the observed value. The predicted minimum refractory time, $(v_{rcc} - v_{exc})/g_{down}$, was 4.3 s.

The automaton presented by Markus and Hess (*10*) was also used to model spiral waves. In this model each Ca^{2+} store was described only by its state variable, S. Upon excitation, a store goes from its ground state $S = 0$ (fully loaded Ca^{2+} store) to the excited state $S = n + 1$ (partially depleted Ca^{2+} store). Thereafter, S decreases by 1 with each iteration. A store was refractory (could not release Ca^{2+}) when S was between S_{max} and n. A store was activated when S was between 0 and S_{max} and when a sufficient number of neighbor stores, within a circle of radius r, were excited. The expression, $m_0 + pS$, described the linear relationship between S and the threshold number of excited neighbors necessary for excitation. Thus, at $S = 0$, m_0 excited neighbors were needed for excitation. The following parameters were used to model the spiral wave: a 50 by 50 grid of Ca^{2+} stores, $r = 4$, $m_0 = 1$, $S_{max} = 4$, $p = 2$, $n = 6$. The velocity of a plane wave, initiated by activating one edge of the grid, was 3.4 stores per iteration. A broken plane wave was used to initiate a spiral that had a period of 7 iterations, and an initial wavelength of 18 stores. When the period of the automaton was set to the experimentally observed value of 10 s, one iteration corresponded to 1.4 s. By equating the automaton's plane velocity to 26 μm/s, one store unit was calculated to be 10.8 μm. The predicted initial wavelength of this automaton (195 μm) differed by less than 8% from the observed value (210 μm). The refractory period, determined from the algorithm of the automaton, $(n + 1 - S_{max})$, was 4.2 s.

13. The linear relation, $N = c - DK$, where N is the normal velocity, c is the planar wave velocity, D is diffusion constant of the excitation signal, and K is the curvature of the propagating wave, was used to estimate D. Measurements of N, c, and K were obtained directly from the data, with no dependence on modeling with cellular automata. J. P. Keener and J. J. Tyson, *Physica*, **21D**, 307 (1986).
14. P. H. Backx *et al.*, *J. Gen. Physiol.* **93**, 963 (1989).
15. M. Whitaker and R. F. Irvine, *Nature* **312**, 636 (1984).
16. P. Foerster, S. C. Muller, B. Hess, *Science* **241**, 685 (1988); *Proc. Natl. Acad. Sci. U.S.A.* **86**, 6831 (1989).
17. An auto-tracing routine (7) was used to define boundaries of equal intensity (>2 intensity units) along all spiral and spherical wavefront patterns of Ca^{2+} release for each optical slice. Regions outside these boundaries were not displayed in order to highlight the patterns of Ca^{2+} release over time. Only the brightest pixel is displayed along the observer's line of sight to add depth to the volume. The intensity scale refers to increases in $[Ca^{2+}]_i$ above resting.

18. We thank C. Bliton and the ANALYZE software support group (Mayo Foundation) for their assistance in imaging, C. Nanavati for assistance in computer modeling, and Dr. P. Camacho for reading the manuscript. Supported by the American Heart Association (J.L. and D.C.), by the Whitaker Foundation (D.C.), and by NIH (E.P. and D.C.).

9 November 1990; accepted 15 February 1991

Mediation of Responses to Calcium in Taste Cells by Modulation of a Potassium Conductance

ALBERTINO R. BIGIANI AND STEPHEN D. ROPER

Calcium salts are strong taste stimuli in vertebrate animals. However, the chemosensory transduction mechanisms for calcium are not known. In taste buds of *Necturus maculosus* (mud puppy), calcium evokes depolarizing receptor potentials by acting extracellularly on the apical ends of taste cells to block a resting potassium conductance. Therefore, divalent cations elicit receptor potentials in taste cells by modulating a potassium conductance rather than by permeating the cell membrane, the mechanism utilized by monovalent cations such as sodium and potassium ions.

RECEPTOR CELLS IN TASTE BUDS sense sodium, potassium, and calcium salts. The discovery that the chemosensitive surface of taste cells has a variety of ion channels has led to a greater understanding of how salts generate receptor potentials (*1*). For example, monovalent cations such as Na^+ and K^+ depolarize receptor cells by entering through specific ion channels in the apical membrane of taste cells (*2, 3*). However, it is still unclear how Ca^{2+} salts, which are powerful and commonly occurring taste stimuli (*4–6a*), are detected. Although voltage-gated Ca^{2+} channels are present in taste cells, they have a relatively high threshold for activation and would not be involved in chemosensory transduction unless taste cells were already depolarized by some other mechanism (*7, 8*).

We have taken advantage of the large taste cells in *Necturus maculosus* (mud puppy) to study chemotransduction mechanisms for Ca^{2+}. Earlier experiments have shown that the mud puppy can taste Ca^{2+} (*9, 10*). We therefore developed a slice preparation of the lingual epithelium (*11*) in which we could visualize and impale single taste cells in isolated living tissue and apply chemical stimuli to the taste pore. Lingual slices containing taste buds were placed in a recording chamber and perfused with amphibian physiological solution (APS) (*12*). Chemosensitivity was studied only in those taste cells that maintained stable resting potentials (−40 to −70 mV) and that responded with action potentials to brief depolarizing cur-

Department of Anatomy and Neurobiology, Colorado State University, Fort Collins, CO 80523, and the Rocky Mountain Taste and Smell Center, University of Colorado Health Sciences Center, Denver, CO 80262.

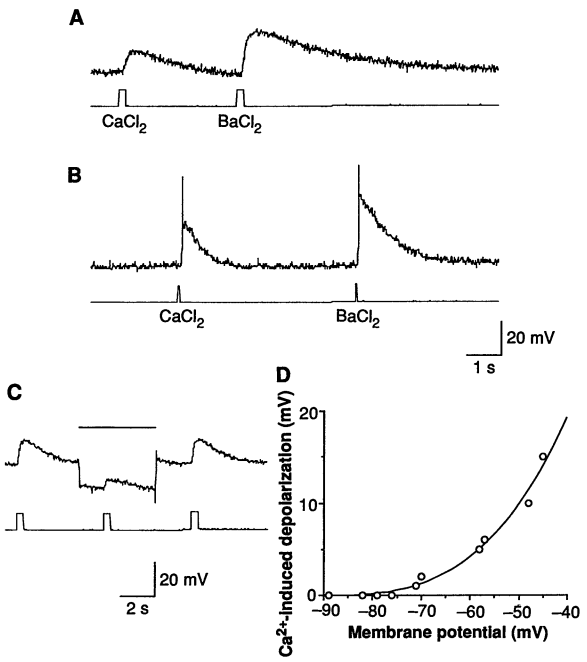

Fig. 1. (**A**) Taste cell responses to $CaCl_2$ and $BaCl_2$, focally applied to the taste pore (resting potential, −51 mV). (**B**) Responses in a different cell. If Ca^{2+} or Ba^{2+} responses were large enough, receptor potentials elicited action potentials (resting potential, −60 mV). Lower traces in (A) and (B) show the pulses of air pressure applied to the barrel of the micropipette containing the chemical stimulus. No responses were detected when the recording microelectrode was situated just outside the taste cell and chemical stimuli were applied. (**C**) Voltage dependence of the amplitude of the receptor potential induced by $CaCl_2$. Responses to $CaCl_2$ at resting potential (−45 mV), at a membrane potential of −58 mV established by passing dc current through the intracellular microelectrode (indicated by the horizontal bar), and again at resting potential. The lower trace monitors the application of $CaCl_2$. (**D**) Amplitude of $CaCl_2$ responses as a function of membrane potential [same cell as (C)]. Solid line, least-squares polynomial fit through the points. Intracellular recordings were obtained with glass micropipettes filled with 2.5 M KCl (90 to 180 megohms). An electrometer with a bridge circuit (WPI M4-A) was used to record the responses and to inject current into the taste cells. Signals were fed into a MacADIOS II GWI-625 data-acquisition board and processed with GWI SuperScope software.

rent pulses (*9, 13*). The $CaCl_2$, $BaCl_2$, and KCl solutions were pressure-ejected from triple-barreled micropipettes, 30 to 50 μm from the taste pore (*14*).

Brief pulses of $CaCl_2$ applied to the taste pore reliably elicited receptor potentials in all taste cells tested (Fig. 1A). If receptor potentials were sufficiently large, they triggered action potentials (Fig. 1B). The amplitudes of receptor potentials evoked by $CaCl_2$ were sensitive to the membrane potential. If the membrane was hyperpolarized below the resting potential, $CaCl_2$ responses were reduced even though the driving force for Ca^{2+} was increased (Fig. 1, C and D). Responses evoked by Ca^{2+} were consistently and reliably abolished at membrane potentials ranging from −75 to −100 mV and did not reverse at more negative membrane potentials (n = 7). In addition, $BaCl_2$ mimicked the effect of $CaCl_2$ on the taste cell apical membrane (Fig. 1, A and B). The Ba^{2+} responses were always larger than the responses evoked by equivalent doses of Ca^{2+} (Fig. 1A).

Voltage-gated Ca^{2+} channels are present in the apical membrane of *Necturus* taste cells (*8, 14a*). To examine whether responses to Ca^{2+} and Ba^{2+} were caused by ion flux through Ca^{2+} channels, we perfused the tissue with Cd^{2+} [a potent Ca^{2+} channel blocker in mud puppy taste cells, even at micromolar concentrations (*7, 8*)]. Receptor potentials evoked by Ca^{2+} and by Ba^{2+} were unaffected by 1 mM $CdCl_2$. Figure 2A illustrates data that are representative of all taste buds that were treated with Cd^{2+} (n = 9). When $CdCl_2$ was included in the stimulating solutions as well as in the bath, we obtained the same result. This experiment was done to verify that applying chemical stimuli did not in itself dilute Cd^{2+} from the apical membrane of taste cells.

Divalent cations, including Ca^{2+}, affect K^+ channels in other cells (*15*). Because the apical membrane of *Necturus* taste cells has a voltage-sensitive resting K^+ conductance (*8, 16, 17*), we studied the effect of tetraethylammonium bromide (TEA), a K^+ channel blocker in mud puppy taste cells (*7, 8, 16*), on responses to $CaCl_2$, $BaCl_2$, and KCl. Responses to focally applied KCl were included to monitor the K^+ conductance of the apical membrane (*8, 16*). As anticipated, TEA (10 mM) completely and reversibly blocked KCl responses. However, TEA also completely and reversibly blocked the responses to $CaCl_2$ and to $BaCl_2$ in all cells tested (n = 9) (Fig. 2B). This result indicated that receptor potentials evoked by Ca^{2+} and Ba^{2+} were mediated by a resting K^+ conductance. Furthermore, Ca^{2+} (and

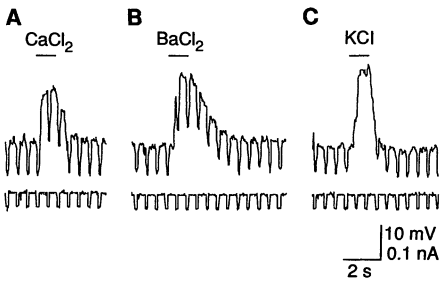

Fig. 3. Change in the input resistance of a taste cell elicited by (**A**) $CaCl_2$, (**B**) $BaCl_2$, and (**C**) KCl (indicated by the horizontal bars) (resting potential, −45 mV). Hyperpolarizing current pulses (lower trace) were injected into the cell through the recording microelectrode. Input resistance increased 67% during the peak of the response to Ca^{2+} (A) and 88% during the peak of the response to Ba^{2+} (B). KCl elicited a 65% reduction in input resistance (C). Whereas the amplitudes of the responses induced by $BaCl_2$ and by KCl were similar, the corresponding changes in the input resistance of the cell were opposite. The decrease in the input resistance during stimulation with KCl is caused by membrane rectification during depolarization and is also observed when the membrane potential is altered by injecting current (*13*).

Ba^{2+}) receptor potentials were associated with an increase in the membrane resistance in taste cells. Figure 3 illustrates representative measurements of input resistance, showing one taste cell that was stimulated sequentially with Ca^{2+}, Ba^{2+}, and K^+. The increases in input resistance elicited by $CaCl_2$ ranged from 43 to 100% (n = 8 cells) and by $BaCl_2$ ranged from 50 to 171% (n = 5 cells). The magnitude of the increase in input resistance depended on several factors, including the dose of applied chemical stimulus, the resting membrane potential, and the resting input resistance.

Our results indicate that the detection of Ca^{2+} occurs through the block of a resting K^+ conductance in taste cells. The voltage dependence of the Ca^{2+} (and Ba^{2+}) responses can be explained as a direct consequence of the voltage sensitivity of the resting K^+ channels: hyperpolarization of the membrane reduces the resting K^+ conductance and thus precludes closure of K^+ channels by Ca^{2+} or Ba^{2+}. Our findings may explain the lack of conductance changes for divalent cations in taste cells reported by others (*4*): increases in membrane conductance are notoriously difficult to detect because they are readily shunted even by slight damage during intracellular impalements. Our results also provide a mechanism for the suggestion that Ca^{2+} salts are adsorbed onto the taste cell membrane to produce their physiological effects (*18*).

The involvement of ion channels other than Ca^{2+} channels may be a general mechanism underlying chemosensitivity to Ca^{2+}

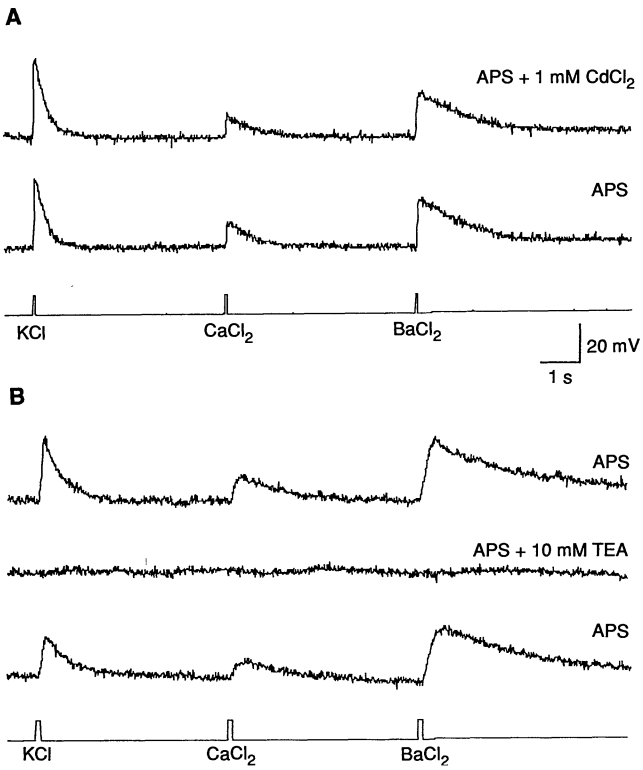

Fig. 2. Effect of ion channel blockers on receptor potentials evoked by focal application of KCl, $CaCl_2$, and $BaCl_2$. (**A**) (Upper trace) Responses in the presence of 1 mM $CdCl_2$ (4 min of Cd^{2+}, bath application). (Bottom trace) Responses 5 min after washing with APS. Records before applying Cd^{2+} (not shown) were identical to these two traces. Resting membrane potential, −47 mV. (**B**) Effect of TEA on receptor potentials in another taste cell. (Upper trace) Responses to KCl, $CaCl_2$, and $BaCl_2$ recorded in APS at resting membrane potential (−53 mV). (Middle trace) Responses during bath application of 10 mM TEA (5 min). TEA produced a 25-mV depolarization in the resting membrane potential [due to blockade of the resting K^+ conductance (*8, 16*)]. We repolarized the membrane to the initial resting value of −53 mV by passing a constant current through the recording electrode so that receptor potentials could be compared at the same membrane potential before and during TEA. Identical results were observed if the membrane was left depolarized (not shown). (Bottom trace) After 3 min of washing in normal APS the membrane potential recovered to the initial resting value. Lower traces in (A) and (B) show the pulses of air pressure applied to the barrel of the micropipette containing the chemical stimulus.

in other tissues, too. For example, in calcitonin-secreting cells from human medullary thyroid carcinoma, increased plasma Ca^{2+} initially depolarizes cells by reducing K^+ or Cl^- conductance. Secondarily, Ca^{2+} influx through voltage-gated Ca^{2+} channels elicits hormone secretion (*19*). Calcium sensitivity in taste cells is similar to glucose sensitivity in pancreatic β cells: the initial depolarization produced by glucose is also caused by a reduction of K^+ conductance (*20*).

In man, Ca^{2+} salts generally produce a salty-bitter taste (*6*). Other taste qualities, including sour and sweet, may also be mediated in part by a modulation of K^+ conductance in taste cells (*16, 17, 21*). However, it is unlikely that a single universal mechanism fully explains chemosensory transduction of such diverse taste qualities, and the mechanism whereby sour, bitter, and sweet sensations are distinguished remains a paradox. Presumably, other changes in addition to alterations in K^+ conductance are involved in generating receptor potentials in different classes of receptor cells. For example, denatonium, an intensely bitter compound in man, blocks K^+ conductance and releases Ca^{2+} from intracellular stores in a subset of cells in taste buds (*22*). Nonetheless, the fact that taste cells have a highly voltage-dependent K^+ conductance that can be modulated by a variety of chemical stimuli imparts a precise voltage sensitivity to taste responses. Small (<10 mV) changes in the resting potential can have a profound effect on the amplitude of receptor potentials by virtue of the voltage sensitivity of the resting K^+ conductance. This property could be an important link between taste sensitivity and metabolic processes that affect resting membrane potential, for example, activity of electrogenic ion transporters such as Na^+,K^+ adenosine triphosphatase, Ca^{2+} exchanger.

REFERENCES AND NOTES

1. S. D. Roper, *Annu. Rev. Neurosci.* **12**, 329 (1989).
2. P. Avenet and B. Lindemann, *J. Membr. Biol.* **112**, 1 (1989).
3. S. S. Schiffman, *Chem. Sens.* **15**, 129 (1990).
4. D. Junge and M. S. Brodwick, *Comp. Biochem. Physiol.* **35**, 623 (1970).
5. T. Sato, *Prog. Neurobiol. (N.Y.)* **14**, 25 (1980).
6. R. W. Moncrieff, *The Chemical Senses* (CRC, Cleveland, 1967).

6a. Y. Kitada, *Jpn. J. Physiol.* **28**, 413 (1978).

7. S. C. Kinnamon and S. D. Roper, *J. Gen. Physiol.* **91**, 351 (1988).
8. S. D. Roper and D. W. McBride, Jr., *J. Membr. Biol.* **109**, 29 (1989).
9. P. Avenet and B. Lindemann, *ibid.* **95**, 265 (1987).
10. M. McPheeters and S. Roper, *Chem. Sens.* **10**, 341 (1985).
11. Mud puppies were rapidly decapitated and the tongues removed. The lingual epithelium was gently freed by blunt dissection and affixed with cyanoacrylic glue to a section of carrot. Thin slices (200 μm) were cut with a tissue chopper while the tissue was kept moist with chilled APS. Slices were scanned, and those containing taste buds were selected for electrophysiological experiments.
12. APS: 112 mM NaCl, 2 mM KCl, 8 mM $CaCl_2$, 5 mM Hepes, buffered to pH 7.2 with NaOH. Elevated Ca^{2+} concentrations facilitated stable intracellular impalements.
13. S. C. Kinnamon and S. D. Roper, *J. Physiol. (London)* **383**, 601 (1987).
14. We prepared chemical stimuli by dissolving $CaCl_2$ (200 mM), $BaCl_2$ (200 mM), and KCl (100 mM) in APS. Ba^{2+} was tested because it mimics the action of Ca^{2+}. KCl is a known stimulus for taste cells and was used both to establish the position of the multibarreled micropipette and to monitor the apical, resting K^+ conductance (*8, 16*). Stimulating solutions were applied focally to the apical membrane of taste cells from triple-barreled micropipettes (tip diameter, 10 to 15 μm). The perfusion system (3 to 5 ml/min) directed APS over the taste bud and thus rapidly removed chemical stimuli after their application to the taste pore (monitored with Fast Green dye). Chemical stimuli were prevented from reaching the basolateral surfaces of the taste cells. The concentration at the apical membrane of the taste cells was lower than the concentration applied as a result of dissipation in the bath. On the basis of the Nernst equation [assuming the intracellular K^+ concentration to be 80 mM (*16*)] and the peak amplitude of KCl responses, we estimated a peak KCl concentration at the taste cell membrane of 20 to 30 mM, corresponding to a three- to fivefold dilution from the concentration in the stimulating pipette. By using this dilution factor for $CaCl_2$ and $BaCl_2$, we calculated their concentrations at the apical membrane to be 40 to 60 mM. These concentrations are higher than those used in taste experiments in the intact animal (*3*). This difference is because tissue slices, especially the apical ends of taste cells, are bathed in a solution of saline that causes adaptation. This raises the threshold of excitation to Ca^{2+} salts (*3, 6a*).

14a. S. C. Kinnamon, T. A. Cummings, S. D. Roper, K. G. Beam, *Ann. N.Y. Acad. Sci.* **560**, 112 (1989).

15. C. M. Armstrong and D. R. Matteson, *J. Gen. Physiol.* **87**, 817 (1986); B. Rudy, *Neuroscience* **25**, 729 (1988); J. B. van de Mortel, A. P. Theuvenet, G. W. Borst-Pauwels, *Biochim. Biophys. Acta* **1026**, 220 (1990).
16. S. C. Kinnamon and S. D. Roper, *Chem. Sens.* **13**, 115 (1988).
17. S. C. Kinnamon, V. E. Dionne, K. G. Beam, *Proc. Natl. Acad. Sci. U.S.A.* **85**, 7023 (1988).
18. N. Akaike, A. Noma, M. Sato, *J. Physiol. (London)* **254**, 87 (1976); K. Kurihara, in *Biosignal Transduction Mechanism*, M. Kasai, T. Yoshioka, H. Suzuki, Eds. (Japan Scientific Society Press, Tokyo/Springer-Verlag, Berlin, 1989), pp. 181–205.
19. O. Sand, L. Jonsson, M. Nielsen, R. Holm, K. M. Gautvik, *Acta Physiol. Scand.* **126**, 173 (1986).
20. F. M. Ashcroft, D. E. Harrison, S. J. H. Ashcroft, *Nature* **312**, 446 (1984).
21. K. Tonosaki and M. Funakoshi, *ibid.* **331**, 354 (1988).
22. M. H. Akabas, J. Dodd, Q. Al-Awqati, *Science* **242**, 1047 (1988); A. I. Spielman *et al.*, *Brain Res.* **503**, 326 (1989).

23. We thank P. Avenet, R. Delay, D. Ewald, and S. Kinnamon for critical review of the manuscript. Supported in part by NIH grants 2 PO1 NS 20486, 5 RO1 AG06557, and 2 RO1 NS24107.

9 November 1990; accepted 1 February 1991

Low-Resolution Real-Space Envelopes: An Approach to the Ab Initio Macromolecular Phase Problem

S. SUBBIAH

An ab initio approach to the phase problem in macromolecular x-ray crystallography is described. A random gas of hard-sphere point scatterers is allowed to condense under the constraint of the solvent fraction and the restraint of the observed Fourier amplitude data. Two applications to real macromolecular examples are discussed. This method produces an approximate outline of the bulk solvent regions and thus yields a low-resolution picture of the unit cell that can be extended to higher resolutions in special cases, such as through the use of molecular replacement or of noncrystallographic symmetry-based phase extension.

THE PHASE PROBLEM IS A SEVERE rate-limiting step in macromolecular x-ray structure determination (*1*). Simply stated, the diffraction pattern of a crystal gives only the amplitudes of the Fourier transform of the crystal contents; the phase angle is lost. In principle, provided enough unique diffraction amplitudes are known, the many constraints imposed by a knowledge of general molecular structure make the inversion of the known Fourier amplitudes, in the absence of any phase information, into real-space electron density an overdetermined problem (*2*). However, theoretical methods, such as the direct method or the Patterson method (*3*), that exploit this overdeterminacy are presently only available for small molecules (typically fewer than 100 nonhydrogen atoms).

Much work has gone into the extension of direct methods to macromolecules (*1*), the exploration of the maximum entropy (ME) method for both the small molecule and macromolecule case (*4*), and the use of simulated annealing in both reciprocal and Patterson space for small molecule test cases (*5*).

Virtually all macromolecular x-ray phases have been obtained by experimental means, such as multiple isomorphous replacement (MIR), MIR supplemented by anomalous scattering data, single isomorphous replacement (SIR) supplemented by anomalous scattering data, and recently the multiple wavelength method when suitable anoma-

Beckman Laboratories for Structural Biology, Department of Cell Biology, Stanford University School of Medicine, Stanford, CA 94305.